



**AUSTRALIAN ATOMIC ENERGY COMMISSION
RESEARCH ESTABLISHMENT
LUCAS HEIGHTS**

**MEASUREMENT OF THE THERMAL NEUTRON WAVE
DISPERSION RELATIONS IN BeO**

by

**A.I.M. RITCHIE
S. WHITTLESTONE**

May 1971

APPROVED FOR PUBLICATION

ISBN 0 642 99416 1

ERRATUM SHEET FOR AAEC/TM591

by

A.I.M. RITCHIE and S. WHITTLESTONE

The density corrections quoted in paragraph 2 page 10 are incorrect. The corrections of the attenuation constant α , the phase shift constant ξ and angular frequency ω measured at density ρ , to the corresponding parameters α_R , ξ_R , ω_R at the reference density ρ_R should have the form

$$\alpha_R = \frac{\rho_R}{\rho} \alpha$$

$$\xi_R = \frac{\rho_R}{\rho} \xi$$

$$\omega_R = \frac{\rho_R}{\rho} \omega$$

Hence $2\alpha\xi$ is proportional to ρ^2 and not ρ as stated.

The entries in Tables 2 and 3 should now read:

Table 2

$$\begin{aligned} P_0 &= (6.477 \pm 0.078) \times 10^{-3} \text{ cm}^{-2} & P_1 &= (6.847 \pm 0.071) \times 10^{-6} \text{ cm}^{-2} \text{ sec} \\ P_2 &= (2.33 \pm 0.25) \times 10^{-10} \text{ cm}^{-2} \text{ sec}^2 & P_3 &= (-0.01 \pm 1.1) \times 10^{-14} \text{ cm}^{-2} \text{ sec}^3 \end{aligned}$$

Table 3

Sine wave results

$$\begin{aligned} \lambda_\alpha &= (1.95 \pm 0.17) \times 10^2 \text{ sec}^{-1} & D_0 &= (1.460 \pm 0.015) \times 10^5 \text{ cm}^2 \text{ sec}^{-1} \\ C &= (7.2 \pm 0.8) \times 10^5 \text{ cm}^4 \text{ sec}^{-1} & L &= (27.4 \pm 1.2) \text{ cm} \end{aligned}$$

Appropriate scaling factors need to be applied to the ordinates and abscissae of the experimental points in Figure 5 and to the abscissae of the experimental points in Figure 6. It should be noted that, making the assumption that one group theory adequately describes the $2\alpha\xi$ curve, the curve presented in Figure 5 yields correctly the density normalised value of D_0 .

The conclusions drawn from the experimental results are not affected by these changes.

AUSTRALIAN ATOMIC ENERGY COMMISSION

RESEARCH ESTABLISHMENT

LUCAS HEIGHTS

MEASUREMENT OF THE THERMAL NEUTRON WAVE

DISPERSION RELATIONS IN BeO

by

A.I.M. RITCHIE

S. WHITTLESTONE

ABSTRACT

The amplitudes and phase shifts of thermal neutron waves were measured in a block of BeO 60.96 x 60.96 x 58.42 cm³ of average density 2.87 g cm⁻³ and having nominal transverse buckling of 0.0048 cm⁻². The attenuation constants (α) and phase shift constants (ξ) were derived from such measurements at 18 different frequencies covering the range 52.4 to 506.1 Hz. The parameters $\alpha^2 - \xi^2$ and $2\alpha\xi$ were evaluated, normalised to a reference density of 2.96 g cm⁻³, and corrected for the density normalised transverse buckling of 0.00513 cm⁻². The normalised and corrected parameters $\alpha^2 - \xi^2$ and $2\alpha\xi$ were fitted to polynomials in the angular frequency ω , and the resulting thermal neutron diffusion parameters were compared with those derived from a $\lambda(B^2)$ experiment carried out on the same block of BeO.

continued ...

ABSTRACT (continued)

The parameters λ_a and L determined by the two methods are in good agreement, but the diffusion coefficient and diffusion cooling constant derived from the sine wave experiment are significantly higher. The high diffusion coefficient (by ~ 9 per cent) could be due to the effect of the sub-Bragg continuum although the values of the parameters α and ξ appeared to be independent of the distance from the source. Agreement of the parameters $\alpha^2 - \xi^2$ and $2\alpha\xi$ with the theoretical values is not good and reasons for the discrepancy are advanced.

Note: This work has been submitted to a journal. Further details can be obtained from the authors or the Director of the Research Establishment.

National Library of Australia card number and ISBN 0 642 99416 1

CONTENTS

| | <u>Page</u> |
|---------------------------------------------------------|-------------|
| 1. INTRODUCTION | 1 |
| 2. EXPERIMENTAL SYSTEM | 2 |
| 3. EXPERIMENTAL METHOD | 3 |
| 4. DATA REDUCTION | 4 |
| 5. DISCUSSION OF ERRORS | 7 |
| 5.1 Errors in Amplitudes and Phases | 7 |
| 5.2 Errors in the Attenuation and Phase Shift Constants | 9 |
| 5.3 Errors in the Diffusion Parameters | 9 |
| 6. RESULTS AND DISCUSSION | 9 |
| 7. CONCLUSIONS | 12 |
| 8. ACKNOWLEDGEMENTS | 13 |
| 9. REFERENCES | 13 |

TABLE 1 Attenuation and Phase Shift Constants for BeO of
 Density 2.87 g cm^{-3}

TABLE 2 Coefficients P_n Derived From a Fit to the Functions
 $\alpha^2 - \xi^2$ and $2\alpha\xi$

TABLE 3 Comparison of the Thermal Neutron Diffusion
 Parameters of BeO

FIGURE 1 Schematic diagram of neutron source and moderator
 assembly

FIGURE 2 Block diagram of time analysis system

FIGURE 3 Typical time distribution and its harmonic analysis

FIGURE 4 The attenuation constant α and phase shift constant ξ
 for BeO of density 2.87 g cm^{-3} as a function of the
 angular frequency ω

FIGURE 5 The quantity $2\alpha\xi$ for BeO, normalised to a density 2.96 g cm^{-3} ,
 as a function of the angular frequency ω

FIGURE 6 The quantity $\alpha^2 - \xi^2$ for BeO, normalised to a density
 2.96 g cm^{-3} , as a function of the angular frequency ω

1. INTRODUCTION

In recent years the sine wave experiment has appeared as a technique complementing the pulsed experiment in investigations of the manner in which neutrons propagate through materials. The technique consists of measuring the amplitude and phase of the sinusoidally modulated neutron density as a function of distance and frequency in the material of interest. Raievsky and Horowitz (1956) were the first to show how the thermal neutron diffusion parameters of a moderator could be derived from such a measurement, and Perez and Uhrig (1963) later indicated the relationship between the parameters measured in the pulsed experiment and those measured in the sine wave experiment.

The analysis of Perez and Uhrig, generalised by the work of Michael and Moore (1967), relied on the assumption that an asymptotic mode could be established in the medium and that for this mode

$$| \kappa v / (i\omega + v\Sigma_t) | \ll 1 \quad \dots(1)$$

where $\kappa = \alpha + i\xi$ the complex propagation constant

α = attenuation constant, and

ξ = phase shift constant.

However in polycrystalline materials the existence of a Bragg cut-off produces a very low value of $(\Sigma_t)_{\min}$ and generally invalidates the assumption (1). For example, in BeO $\kappa \sim 0.038 \text{ cm}^{-1}$ at zero frequency and zero transverse buckling whereas the minimum value of Σ_t is about 0.03 cm^{-1} . Duderstadt (1968) pointed out that the relationship (1) was not generally valid in polycrystals and further showed that the eigenvalue spectrum of the operator in the Boltzmann equation, which described sine wave pulsing in a polycrystalline moderator, consisted of four parts: a discrete spectrum which normally describes the asymptotic mode, a sub-Bragg continuum, an elastic continuum and an area continuum. An important part of his analysis was the finding that the minimum value of α associated with the sub-Bragg continuum could, in some cases, be less than the value of α associated with the lowest discrete mode. This meant that the sub-Bragg continuum could dominate at sufficiently large distances from the source and that the attenuation and phase shift 'constants' would change with distance from the source. This prediction was a generalisation of a similar prediction about the static diffusion length experiment made by Williams (1968) who showed that in many moderator assemblies with sizeable transverse leakage no discrete mode existed.

A number of sine wave experiments have been reported in graphite (Utsuro et al. 1968, Takahashi and Sumita 1968, Perez and Booth 1965), but none in BeO or Be. Since a sample of BeO has been studied in some detail (Ritchie 1968a, and

Rainbow and Ritchie 1968) by the pulsed technique, it was thought useful to study the same sample by the sine wave technique. In this sample of BeO the reciprocal of the diffusion length (α at zero frequency and zero transverse buckling) is 0.038 cm^{-1} , which is somewhat larger than the value of 0.03 cm^{-1} for the total cross section just below the Bragg cut-off. Hence contribution from the sub-Bragg continuum could be expected. Duderstadt has also indicated that the curve representing the dispersion relationship for the discrete mode intersects the bounding curve of the elastic continuum at an angular frequency

$$\omega \sim (v\Sigma_t)_{v=v_B}$$

where v_B is the velocity corresponding to the Bragg cut-off. In the present sample of BeO $(v\Sigma_t)_{v=v_B}$ is estimated to be 2750 s^{-1} which corresponds to a frequency of 440 Hz. For this reason it was decided to explore the frequency range 0-500 Hz. It was also decided to use a sine wave source rather than make use of the pulse propagation technique in order to simplify data analysis and to clarify interpretation of data in the event of significant contributions from the various continua.

2. EXPERIMENTAL SYSTEM

Neutrons were produced by bombarding a suitable target with protons or deuterons accelerated by a 3 MeV Van de Graaff accelerator. The charged particle beam passed through a set of electrostatic deflection plates which deflected the beam on and off an aperture placed some 4 metres in front of the target, so allowing modulation of the beam intensity at the target. Sine wave modulation was produced by comparing a signal derived from the target with that from a sine wave generator and feeding a suitable error signal back to the deflection plates. The details of this system are given by Fraser et al. (1968).

The ideal sine wave neutron source for a neutron wave experiment has a high proportion of thermal neutrons, high intensity and a large modulation depth. The system outlined above can provide an intense source of neutrons with a large modulation depth, but since neutrons from the most useful charged particle reactions have energies in the MeV region a moderator, which unfortunately attenuates the oscillatory component of the neutron source, must be used to slow the neutrons down to thermal energies. The more moderator used the higher the thermal neutron intensity but the lower the modulation depth. Hence it is necessary to compromise between high thermal neutron intensity and large modulation depth. A similar compromise is necessary in choosing the most suitable charged particle reaction.

The most copious neutron producing reaction available on a 3 MeV Van de Graaf is the $^9\text{Be}(d,n)^{10}\text{B}$ reaction which provides a source of predominantly 2 MeV neutrons at a deuteron energy of 2.8 MeV, but with some neutron energies ranging up to about 7 MeV (Inada et al. 1968). The $^7\text{Li}(p,n)^7\text{Be}$ reaction, on the other hand, is not such an intense source, but at a proton energy of 2 MeV the neutrons have energies of only about 100 keV and hence are more easily thermalised (particularly in a hydrogenous moderator) than those from the $^9\text{Be}(d,n)^{10}\text{B}$ reaction.

Several preliminary experiments were done using these two reactions and a variety of moderators (iron, graphite, polythene) in a number of different configurations. The best compromise was obtained using a slab of polythene 3 inches thick together with a thick (~ 500 keV) lithium target and a proton energy of 2.4 MeV to produce neutrons with a maximum energy of about 500 keV. The bulk of the work was carried out using a 50 μA proton beam and a modulation depth of 90 per cent with about 2 per cent harmonic distortion.

Since both the neutron intensity and neutron energy from the $^7\text{Li}(p,n)^7\text{Be}$ reaction change rapidly with changes in the proton energy, it is important to stabilise the accelerator voltage. The system used to do this was based on the generating voltmeter installed on the machine and controlled the machine voltage to ± 2 kV. More details of the preliminary experiments and the stabilisation system are given by Whittlestone (1968).

The BeO consisted of tiles $15.24 \times 15.24 \times 2.54$ cm³ which were stacked in the form of a parallelepiped $60.96 \times 60.96 \times 58.42$ cm³ in which there was a probe hole 1.02×1.02 cm² running parallel to the z-direction at the point $x = 10.16$ cm, $y = 0.0$ cm (see Figure 1). The details of the clamping arrangement and the shielding are essentially the same as those given by Ritchie (1968a). The lithium target was placed some 30 cm in front of the BeO at the centre of the 60.96×60.96 cm² face as a simple calculation showed that this resulted in spatial distribution in the x and y directions that was closest to a cosine. A cadmium shutter was interposed between the polythene and BeO to provide a means of estimating the fast neutron component of the source.

3. EXPERIMENTAL METHOD

A block diagram of the detection and time analysis system is shown in Figure 2. The master instrument was the sine wave generator which, as well as providing a comparison signal for the sine wave source, provided timing pulses at the start of each cycle. These timing pulses were fed through a divide-by-two network, then fed as start pulses to the time analysers. This meant that the time distributions from the detectors were measured over almost two complete cycles, which permitted more accurate estimation of the harmonic content. The timing pulses also controlled a reversible scaler which added input pulses from the monitor detector

during the first half-cycle and subtracted input pulses during the second half-cycle, so giving, in the absence of higher frequency mode contamination, the amplitude of the fundamental mode. This reversible scaler was used to normalise each time distribution measurement to a nominally constant fundamental component in the monitor detector by closing gates on the inputs to the two time analysers after a preset count had been reached. Because of higher mode contamination this normalisation was only approximate, but was useful as a minute-to-minute check on runs during the experiment. The time-averaged levels of both the movable and monitor detector time distributions were measured by scaling the outputs of these two detectors.

The flux distribution in the beam, or z-direction, was measured using a 20th Century 1/4 inch BF_3 detector which was positioned by means of the counter drive system described previously (Ritchie 1968b). Another 1/4 inch BF_3 detector, clad in cadmium and placed in the middle of the polythene slab, acted as monitor. The pulses from both these detectors were fed, via fairly standard amplifying and pulse shaping units, into two time analysers, namely a modified Laben 512-channel analyser (Ritchie 1968a) and a PDP-7 computer fitted with an ancillary time analysis unit (Rainbow and Ritchie 1970). Both analysers were used with 32 channels as this provided good counting statistics and more than adequate time points for the analysis of the higher mode contamination in the time distributions.

Eighteen frequencies in the range 52.4 to 506.1 Hz were investigated. At each frequency the time distribution of the movable detector was measured at 15 equally spaced points in the range $z = 7.75$ to 49.75 cm, a run with the cadmium shutter out being alternated with a run with the cadmium shutter in. The channel widths in the time analysers varied from $1170 \mu\text{s}$ in the 52.4 Hz run to $120 \mu\text{s}$ in the run at 506.1 Hz. A measurement of the transverse buckling was also carried out by measuring the spatial distribution at zero frequency in the y-direction with $x = -0.508$ cm, $z = 29.2$ cm and y varying from 22.9 to -27.1 cm by steps of 10 cm.

4. DATA REDUCTION

There were three major steps in the analysis of the experimental time distributions:

- (i) Extraction of the amplitudes and phase shifts at each position.
- (ii) Evaluation of the attenuation and phase shift constants from the amplitudes and phases as a function of distance.
- (iii) Evaluation of the thermal neutron diffusion parameters from the attenuation and phase shift constants.

Both the monitor and movable detector time distributions were fitted to the following expression:

$$y(t) = \sum_{n=1} E_n \cos n\omega t + \sum_{n=1} F_n \sin n\omega t + E_0 ,$$

using a weighted least squares criterion to determine the best fit to the data. Amplitudes A_n and phase shifts ψ_n of the n^{th} harmonic were then evaluated from the E_n and F_n using the formulae:

$$A_n = \sqrt{E_n^2 + F_n^2}$$

$$\psi_n = -\tan^{-1} F_n/E_n$$

Figure 3 shows a typical time distribution and the amplitudes and phase shifts required to fit it. In general the time-averaged amplitude E_0 and the first four frequency harmonics were found sufficient to fit the time distributions. The amplitudes of the harmonics in the movable detector time distribution were normalised using the amplitude of the lowest harmonic in the monitor time distribution.

In finding the attenuation and phase shift constants associated with the fundamental frequency the flux in the assembly was assumed to have the form

$$\phi(z,t) = \Re y_0 \{ \exp(-(\alpha + i\xi)z) - \exp(\alpha + i\xi)(z - 2C) \} \exp i\omega t \quad \dots(2)$$

$$= \Re y(z, \alpha, \xi) \exp i\omega t \quad , \quad \dots(3)$$

where α = attenuation constant,
 ξ = phase shift constant, and
 C = extrapolated length in the z direction.

This can be written as

$$\phi(z,t) = A(z) \Re \exp i\psi(z) \exp i\omega t \quad \dots(4)$$

$$= \Re Y(z, A(z), \psi(z)) \exp i\omega t \quad , \quad \dots(5)$$

where $A(z)$ = amplitude of the fundamental wave
and $\psi(z)$ = phase shift of the wave at the point z .

Now $A(z)$ and $\psi(z)$ are the quantities measured experimentally, and it should be noted that in an assembly of finite size both are functions of the phase shift constant ξ and the attenuation constant α . For example

$$A(z) = y_0 \exp(-\alpha C) \sqrt{2 \cosh 2\alpha(z-C) - 2 \cos 2\xi(z-C)}. \quad \dots(6)$$

Hence it is necessary to find the values of α and ξ which simultaneously give the best fit to the observed phase shifts and amplitudes.

A weighted least squares method was used to fit the experimental data with the form (2). The actual form of the function to be minimised follows from expressions (2) and (4) and is most concisely expressed in terms of (3) and (5) as

$$\chi^2 = \sum_i w_i (\Re y_i - \Re Y_i)^2 + \sum_i W_i (\Im y_i - \Im Y_i)^2 \quad \dots(7)$$

The weights w_i and W_i were derived from the experimental errors on the amplitudes and phases at the point z_i and expressions of the form (6). The equations determining the values of α and ξ which minimise the function (7) are non-linear in α and ξ and require some iteration method to solve them. An iteration method, developed from that described by Powell (1968), has proved both fast and trouble-free.

The values of α and ξ were used to evaluate the quantities $\alpha^2 - \xi^2$ and $2\alpha\xi$. These, following Perez and Uhrig (1963), were then fitted to the power series

$$\begin{aligned} \alpha^2 - \xi^2 &= \sum_{n=0}^{\infty} P_{2n} (i\omega)^{2n} \\ 2\alpha\xi &= \sum_{n=0}^{\infty} P_{2n+1} \omega^{2n+1} i^{2n} \end{aligned} \quad \dots(8)$$

In practice both $\alpha^2 - \xi^2$ and the quantity $2\alpha\xi/\omega$ were fitted with power series in ω^2 using a standard least squares method. The thermal neutron diffusion parameters were then derived (see Perez and Uhrig 1963, Michael and Moore 1967) from the coefficients P_n ; for example the coefficient

$$D_0 = P_1^{-1} \text{ cm}^2 \text{ sec}^{-1} \quad \dots(9)$$

and the diffusion cooling constant

$$C = P_2/P_1^3 \text{ cm}^4 \text{ sec}^{-1} \quad \dots(10)$$

In particular, the diffusion length L was determined from the zero intercept α_0 of α as a function of ω and the relationship

$$1/L^2 = \alpha_0^2 - B_1^2, \quad \dots(11)$$

where B_1^2 was the transverse buckling.

5. DISCUSSION OF ERRORS

5.1 Errors in Amplitudes and Phases

The errors in the amplitude and phase at any one point were compounded from the following:

- (i) Errors in the time distributions.
- (ii) Changes in the detection efficiency of the detection system.
- (iii) Changes in the space-energy distribution of the neutron flux in the assembly.
- (iv) Errors in positioning the movable detector.

The only errors assumed in the time distribution were those due to random errors in counting, since these varied from 0.2 to 1 per cent and far outweighed the timing errors, estimated to be 0.01 per cent. The errors in the amplitudes and phases were extracted from the weighted least squares fitting routine in the standard manner and varied between 0.15 and 5 per cent over the frequency range 50 to 500 Hz.

Changes in detection efficiency can be caused by changes in E.H.T., drift in amplifier gain, drift in discriminator level and those changes in efficiency at high count rate which can most conveniently be described by a dead time. The variation due to drifts in E.H.T., amplifier gain and discriminator level were estimated at less than 0.04 per cent and were neglected. The change of efficiency at high count rate, largely attributed to base line shifts in the electronics, was much more significant and a possible source of systematic error. It is reasonable to expect this change in efficiency to be an approximately linear function of the count rate similar to that associated with a 'dead time', that is

$$N = N_0 / (1 - \tau N_0),$$

where N = correct count rate,
 N_o = observed count rate,
 τ = composite 'dead time' parameter.

The parameter was found by observing the count rate from one detector at two high and markedly different count rates. The count rate was increased by increasing the beam current from the accelerator, the actual count rate being estimated from a monitor placed sufficiently far from the source for 'dead time' effects to be negligible. The values of the 'dead times' found for the monitor and movable detector were 5.7 and 2.0 μ s respectively and gave rise to corrections of up to 6 per cent in some time channels. As a check that there was negligible systematic error, the time distribution at an arbitrarily picked spatial point at each frequency was repeated at a count rate decreased by a factor of two from that used throughout most of the runs. No systematic differences in the amplitudes and phases outside the errors were found during these runs after the 'dead time' correction had been applied.

Changes in the space energy distribution of the neutron flux were assumed attributable to changes in the energy of the proton beam, to movement of the beam spot on the target, to inaccuracy in positioning the cadmium shutter and to changes in thickness of the lithium target. The primary effect of all of these was a change in the ratio of detector to monitor counts which led to uncertainties in the amplitude rather than the phase of the wave. The change in the ratio of monitor to detector counts and hence the change in the normalised amplitude as the proton energy changed was found to be 0.05 per cent/keV. This, since the accelerator voltage was stabilised to ± 2 kV, implied 0.1 per cent error in the normalised amplitudes. A similar error of 0.1 per cent was associated with the movement of the beam spot which was measured as less than ± 1 mm. The error in the amplitudes arising from variation in the two rest positions of the cadmium shutter was estimated by noting changes in the count rate of the movable detector when the shutter was moved about these two positions. These errors were 0.015 per cent at the lower position and 0.15 per cent at the upper position. The effects of possible changes in the energy spectrum of neutrons emitted from the target as it decreased in thickness during the experiment were neglected as no corresponding drop in the neutron yield from the target was noted.

The error in positioning the detector was ± 0.3 mm. This gave rise to errors of between 0.25 and 0.35 per cent in amplitude and between 0.05 and 0.25 per cent in phase over the frequency range 50 to 500 Hz.

The total error in the amplitude and phases from the above causes ranged from 0.4 to 5 per cent over the frequency range investigated. However, although the more precise measurements of amplitude agreed within about 0.4 per cent when

repeated within an hour or so, they agreed only within about 1 per cent when repeated after a delay of four to eight hours. In the light of this the lower limit of the error in the amplitudes was increased to 1 per cent.

5.2 Errors in the Attenuation and Phase Shift Constants

The random errors in the attenuation constant α and the phase shift constant ξ were assumed to arise only from the errors in the amplitudes and phases at each space point and were evaluated in the least squares fitting routine that derived α and ξ from the amplitudes and phases as a function of distance.

There were two major sources of systematic error, one associated with the existence of higher spatial modes, the other with changes in the energy distribution along the stack. Measurements of the transverse spatial distribution near the source ($z = 3.8$ cm) showed that, compared to a cosine, the flux was depressed at the centre (about 10 per cent third spatial harmonic contamination). The decay of these higher spatial modes away from the source could lead to a systematically smaller value of the attenuation constant if points close to the source were included in the analysis. A systematic error in the same direction could occur if points were included from the region in which slowing down effects in the sub-cadmium component of the source were significant, since the efficiency of BF_3 detectors increases with decreasing neutron energy.

The systematic error from these two sources can be estimated by evaluating α and ξ from a set of measurements close to the target and a set further away from the target. The set closest to the source ranged from 9 to 30 cm and the set far from the source from 21 to 42 cm. There was no discrepancy between the parameters α and ξ using these two sets.

5.3 Errors in the Diffusion Parameters

The errors in the quantities $\alpha^2 - \xi^2$ and $2\alpha\xi$ were estimated from the values of α and ξ using standard techniques. The errors in the P_n of equation (8) were estimated from the least squares fit to a power law in the usual way and the errors in the diffusion parameters were estimated from expressions of the form (9) and the errors in P_n .

6. RESULTS AND DISCUSSION

Table 1 lists the eighteen frequencies investigated and the values of the phase shift and attenuation constants α and ξ .

The results for α and ξ are those evaluated from spatial points lying between 21 and 42 cm from the source. As indicated in Section 5.2 above, they are apparently independent of the range of distances from the source over which the measurements were carried out, for distances greater than about 9 cm. However, since in BeO the lowest attenuation constant associated with the sub-Bragg

continuum is less than that associated with the lowest discrete mode, the sub-Bragg continuum should dominate at large distances from the source, and the effective values of α and ξ should change with distance. Therefore either the source conditions are such that the contribution from the sub-Bragg continuum is too low to be significant, or else in the spatial region investigated, the discrete mode, sub-Bragg continuum and elastic continuum combine to give a mode of propagation which is not significantly different from a discrete mode. Thus the distance range over which the present values of α and ξ were determined has been given in some detail; this range was chosen to be as far as practical from the source to obtain the maximum contribution from the sub-Bragg continuum.

The parameters α and ξ are plotted as functions of frequency in Figure 4 where they are compared with values of α and ξ estimated from one-group theory using the values of the coefficients D_0 and $\sqrt{\Sigma_\alpha}$ found for the same block of material by the pulsed method. It should be emphasised that the parameters in this figure are referred to the experimental density, $\rho = 2.87 \text{ g cm}^{-3}$, and not $\rho = 2.96 \text{ g cm}^{-3}$, since the parameters α and ξ do not depend simply on the density, unlike the parameters $\alpha^2 - \xi^2$ (proportional to ρ^2) and $2\alpha\xi$ (proportional to ρ).

Curves of $2\alpha\xi$ and $\alpha^2 - \xi^2$ normalised to $\rho = 2.96 \text{ g cm}^{-3}$ and corrected for the normalised transverse buckling of $(5.13 \pm 0.09) \times 10^{-3} \text{ cm}^{-2}$ are shown in Figures 5 and 6. Also shown in these figures are some theoretical curves from the work of Wood (1969a) and some based on one-group theory using parameters derived from the pulsed experiment (Ritchie 1968a). Figure 5 shows that Wood's calculations overestimate the slope of the $2\alpha\xi$ curve by 15 per cent, while the agreement between the one-group theory and experiments is much better. This is to be expected since one-group theory shows the slope of the $2\alpha\xi$ curve is $1/D_0$ while the slope of the $\lambda(B^2)$ curve is just D_0 . The overestimate by Wood is not too surprising in view of the way similar calculations (Wood 1969b, Tewari and Trikha 1968) have underestimated the slope of the $\lambda(B^2)$ curve. Ritchie et al. (1970) showed that when the elastic cross section was corrected for the extinction effects likely to occur in the crystallites of the BeO sample (Zhezherun et al. 1964) the coefficient D_0 was increased by about 10 per cent and better agreement was obtained between the theoretical and experimental $\lambda(B^2)$ curves. A similar correction to the elastic cross section used in Wood's calculation of $2\alpha\xi$ would increase D_0 and improve the agreement between theory and experiment.

It is at once obvious from Figure 6 that one-group theory gives a poor fit to the experimental $\alpha^2 - \xi^2$ curve, as expected since one-group theory is correct only to zero order in the frequency. The second order term, according to the perturbation approach of Perez and Uhrig (1963) is of the form $\omega^2 C/D_0^3$, where C is the diffusion cooling constant of the $\lambda(B^2)$ curve and reflects the departure of the energy spectrum from a Maxwellian. Since C contains a term which depends on

the second moment of the scattering kernel, the departure of $\alpha^2 - \xi^2$ from the one-group result is quite sensitive to the phonon frequency distribution used to describe normal modes of vibration in the BeO. This can be seen from the calculations of Wood (1969a) in which three different phonon frequency distributions were used. Of these, the calculation using a Debye spectrum with $\theta_D = 855^\circ\text{K}$ (curve C in Figure 6) is closest to the experimental data. That using $\theta_D = 1200^\circ\text{K}$ is little different from the curve obtained using Sinclair's $\rho(\beta)$ (curve A in Figure 6) and overestimates the experimental values of $\alpha^2 - \xi^2$.

The reasonable agreement with experiment of the theoretical $\alpha^2 - \xi^2$ curve based on the Debye spectrum with $\theta_D = 855^\circ\text{K}$, is somewhat misleading. If the D_0 value associated with Wood's calculations were increased to improve the agreement between the theoretical and experimental $2\alpha\xi$ curves, there would be a marked change in the associated theoretical $\alpha^2 - \xi^2$ curve. For example if Wood were to take extinction effects into account, D_0 would increase by about 10 per cent, but the coefficient of ω^2 in the $\alpha^2 - \xi^2$ curve would change by about 30 per cent. Thus the $\alpha^2 - \xi^2$ curve based on the $\theta_D = 855^\circ\text{K}$ spectrum would fall below the experimental points, while the curve based on Sinclair's frequency spectrum would show better agreement with experiment. This ability to obtain essentially a diffusion parameter (D_0) from the $2\alpha\xi$ curve and a thermalisation parameter (C) from the $\alpha^2 - \xi^2$ curve is an advantage of the sine wave experiment over the pulsed experiment.

Table 2 lists the coefficients of ω^{2n} and ω^{2n+1} obtained when $\alpha^2 - \xi^2$ and $2\alpha\xi$ were fitted with polynomials in ω . In each case a two parameter polynomial provided the best fit to the data. Such a fit to a power law in ω is valid, but as has been pointed out by Duderstadt (1968) the interrelations (Perez and Booth 1965, Michael and Moore 1967) between these coefficients and those derived from a $\lambda(B^2)$ curve are not valid since the condition $|\kappa v / (i\omega + v\Sigma_t)| \ll 1$ does not hold for all energies in polycrystals in general and BeO in particular. However, for the sake of completeness the parameter λ_a , the coefficient D_0 , the diffusion cooling constant C and the diffusion length L have all been derived from the polynomial coefficients and compared with those parameters derived from the pulsed experiment (see Table 3). There is good agreement between the parameters λ_a and L, but D_0 and C are significantly larger in the case of the sine wave experiment. This is also shown by Figure 5, where the slope of the $2\alpha\xi$ curve derived from the pulsed parameter is greater than that of the present experimental results.

The fact that the value of D_0 found in the wave experiment was high by about 9 per cent could indicate either that intercomparison with the pulsed experiment is invalid since $|\kappa v / (i\omega + v\Sigma_t)| \sim 1$ for velocities just below the Bragg cut-off or that there was some contribution from the sub-Bragg continuum. Such a contribution would weight the energy spectrum towards a region of large mean free path and produce an effective D_0 greater than that associated with the discrete

mode. The good agreement of the parameter λ_a from the two measurements is consistent with the perturbation treatment of Michael and Moore (1967) which shows λ_a is independent of any continuum contribution if Σ_a varies as $1/v$. Similarly the parameter L from the wave experiment should be higher than the pulsed experiment if there is any continuum contribution. This is so, but the difference between the two results is not significantly larger than the errors.

7. CONCLUSIONS

The experimental results for α and ξ were found to be independent of the distance from the source for distances greater than 9 cm. This suggests that an asymptotic mode existed over the spatial range investigated in the BeO sample. However, the markedly high (by about 9 per cent) value of the parameter D_0 derived from the sine wave results compared to that derived from a pulsed experiment in the same sample of BeO, indicates that either the diffusion coefficients derived from the two experiments are not really comparable, or that an asymptotic mode was not in fact established. Both effects are probably present, since in BeO both $|\kappa v / (i\omega + v\Sigma_t)| \sim 1$ at $v = v_B$ and the smallest attenuation rate of the sub-Bragg continuum is less than that of the discrete mode.

In view of the possible contribution from the sub-Bragg continuum the present results should be interpreted as measurements of the effective phase shift and attenuation constants of a predominantly thermal neutron wave in BeO. An adequate theoretical analysis probably requires that the actual experimental geometry and source conditions be taken into account.

Because of the uncertainty in comparing parameters derived from expansion of α and ξ in terms of the frequency with those derived from the expansion coefficients of the buckling B^2 in the $\lambda(B^2)$ relationship, there seems little point in generating the relationships $2\alpha\xi$ and $\alpha^2 - \xi^2$ when comparing experimental and theoretical results. They only help in semi-quantitative judgements on whether the elastic part (from $2\alpha\xi$) or the inelastic part (from $\alpha^2 - \xi^2$) of the cross sections used in the theoretical calculations is more correct. In general it would be more profitable to compare directly theoretical values of the amplitude and phase at any point for a given frequency with the corresponding experimental values; the quantities α and ξ should be used to parameterise the amplitude and phase only when the parameterisation can be done unambiguously. For example the amplitudes and phase shifts could be estimated from space-time distributions synthesised using all (or as many as deemed necessary) of the eigenfunctions of multigroup diffusion theory. Such an approach, which has already been used by Wood (1969c) in some graphite studies, could take explicit account of the energy sensitivity of the detector and of the energy dependence of the source used in the experiment.

The poor agreement of Wood's (1969a) curve for using an elastic cross section based on scattering by ideal polycrystalline BeO, and the much better agreement obtained using simple one-group theory and the parameters derived from a $\lambda(B^2)$ experiment in the same sample of BeO, indicates that the cross section used by Wood is inadequate. Ritchie et al. (1970) showed that good agreement could be obtained with the $\lambda(B^2)$ curve for this sample of BeO when the elastic cross section was modified to allow for extinction in the crystallites of the sample. Any real attempt to obtain good quantitative agreement between theory and experiment should take detailed account of the physical nature of the sample being investigated. In this particular case the change in the parameter D_0 is about 10 per cent, which is much greater than the experimental error of about 1 per cent usually assigned to this quantity in a pulsed or sine wave experiment.

8. ACKNOWLEDGEMENTS

We would like to thank the operating team of the A.A.E.C. 3 MeV van de Graaf accelerator for their assistance during the experiment. In particular we would like to thank Mr. K.J. Maher and Mr. G.D. Trimble for their considerable help in the data analysis.

9. REFERENCES

- Duderstadt, J.J. (1968). - Nucl. Sci. Eng. 33, 119.
- Fraser, H.J., Ritchie, A.I.M. and Whittlestone, S. (1968). - Rev. Scient. Instrum. 39, 240.
- Inada, T., Kowachi, K. and Hiramoto, T. (1968). - J. Nucl. Sci. and Tech. 5, 22.
- Michael, P. and Moore, M.N. (1967). - Proc. Symp. on Neutron Thermalisation and Reactor Spectra, I.A.E.A. Vienna, Vol. 1, p.143.
- Perez, R.B. and Uhrig, R.E. (1963). - Nucl. Sci. Eng. 17, 90.
- Perez, R.B. and Booth, R.S. (1965). - Proc. I.A.E.A. Conf. on Pulsed Neutron Research, Karlsruhe, Vol. 2, p.656.
- Powell, M.J.D. (1968). - U.K.A.E.A. Research Group Report, A.E.R.E. R5947.
- Raievsky, V. and Horowitz, J. (1956). - Proc. of Conf. on Peaceful Uses of Atomic Energy, Geneva, 5, 42.
- Rainbow, M.T. and Ritchie, A.I.M. (1968). - J. Nucl. Energy, 22, 735.
- Rainbow, M.T. and Ritchie, A.I.M. (1970). - Report No. AAEC/TM548.
- Ritchie, A.I.M., Maher, K.J. and Trimble, G.D. (1970). - J. Nucl. Energy, 24, 151.
- Ritchie, A.I.M. (1968a). - J. Nucl. Energy, 22, 371.
- Ritchie, A.I.M. (1968b). - J. Nucl. Energy, 22, 717.
- Takahashi, A. and Sumita, K. (1968). - J. Nucl. Sci. Technol. 5, 7.
- Tewari, S.P. and Trikha, S.K. (1968). - J. Nucl. Energy, 22, 569.
- Utsuro, M., Inoue, K. and Shibata, T. (1968). - J. Nucl. Sci. Technol. 5, 298.
- Whittlestone, S. (1968). - M.Sc. Thesis, University of New South Wales, Australia.

Williams, M.M.R. (1968). - J. Nucl. Energy, 22, 153.

Wood, J. (1969a). - J. Nucl. Energy, 23, 211.

Wood, J. (1969b). - Brit. J. Appl. Phys. (J. Phys. D.) 2, 149.

Wood, J. (1969c). - J. Nucl. Energy, 23, 71.

Zhezherun, I.F., Sadikov, I.P., Tarabanko, V.A. and Chernyshov, D.D. (1964). -
Proc. 3rd United Nations Conf. on Peaceful Uses of Atomic Energy,
Geneva, United Nations, 3, 260.

TABLE 1

Compilation of attenuation and phase shift constants for BeO
of density 2.87 g cm^{-3} for points lying between 21 and 42 cm from the source

| Frequency | | $\alpha \text{ cm}^{-1}$ | $\Delta\alpha \times 10^4$ | $\xi \text{ cm}^{-1}$ | $\Delta\xi \times 10^4$ |
|-----------|-----------------------|--------------------------|----------------------------|-----------------------|-------------------------|
| Hz | rad sec ⁻¹ | | | | |
| 0.0 | 0 | 0.0772 | 10 | | |
| 52.4 | 329 | 0.0800 | 10 | 0.0130 | 2 |
| 103.4 | 650 | 0.0837 | 10 | 0.0261 | 2 |
| 109.9 | 691 | 0.0840 | 10 | 0.0269 | 3 |
| 159.5 | 1002 | 0.0862 | 10 | 0.0370 | 4 |
| 201.2 | 1264 | 0.0920 | 10 | 0.0460 | 4 |
| 229.3 | 1441 | 0.0952 | 10 | 0.0501 | 5 |
| 260.6 | 1637 | 0.0990 | 10 | 0.0559 | 4 |
| 292.9 | 1840 | 0.1020 | 10 | 0.0595 | 5 |
| 304.5 | 1913 | 0.1020 | 10 | 0.0608 | 5 |
| 306.7 | 1927 | 0.1032 | 10 | 0.0609 | 5 |
| 326.0 | 2048 | 0.1076 | 12 | 0.0644 | 8 |
| 354.0 | 2224 | 0.1105 | 12 | 0.0665 | 8 |
| 387.0 | 2431 | 0.1130 | 14 | 0.0719 | 8 |
| 420.7 | 2643 | 0.1180 | 16 | 0.0768 | 8 |
| 453.9 | 2852 | 0.1180 | 20 | 0.0796 | 8 |
| 484.8 | 3046 | 0.1210 | 20 | 0.0830 | 10 |
| 506.1 | 3180 | 0.1220 | 30 | 0.0842 | 15 |

TABLE 2

Coefficients P_n derived from a fit to the functions $\alpha^2 - \xi^2$
and $2\alpha\xi$ with a two-parameter polynomial, normalised to density 2.96 g cm^{-3}

| Fit to the Function $\alpha^2 - \xi^2$ | | Fit to the Function $2\alpha\xi$ | |
|----------------------------------------------|----------------------------------|----------------------------------------------|-----------------------------------|
| $P_0 \text{ (cm}^{-2}\text{)}$ | $(6.48 \pm 0.07) \times 10^{-3}$ | $P_1 \text{ (cm}^{-2} \text{ sec)}$ | $(6.73 \pm 0.06) \times 10^{-6}$ |
| $P_2 \text{ (cm}^{-2} \text{ sec}^2\text{)}$ | $(2.5 \pm 0.3) \times 10^{-10}$ | $P_3 \text{ (cm}^{-2} \text{ sec}^3\text{)}$ | $(0.21 \pm 0.15) \times 10^{-13}$ |

TABLE 3

Comparison of the thermal neutron diffusion parameters of BeO, normalised to a density of 2.96 g cm^{-3} and temperature of 22°C , measured by the pulsed and sine wave methods on the same block of material

| Reference | $\lambda^a (\text{sec}^{-1}) \times 10^{-2}$ | $D_{01} (\text{cm}^2 \text{sec}^{-1}) \times 10^5$ | $C (\text{cm}^4 \text{sec}^{-1}) \times 10^{-5}$ | $L (\text{cm})$ | $\epsilon (\text{cm})$ | Experimental Conditions |
|--------------------------------|----------------------------------------------|----------------------------------------------------|--------------------------------------------------|------------------|------------------------|----------------------------------------------------------------------------------------------------------------------------------------------------|
| Ritchie (1968a) (pulsed) | 1.954 ± 0.076 | 1.343 ± 0.011 | 4.88 ± 0.31 | 26.22 ± 0.51 | | Mean $\rho = 2.867 \text{ g cm}^{-3}$, temp. 22°C $B_1^2 \leq B_2^2 \leq 0.028 \text{ cm}^{-2}$ |
| Present results (sine wave) | 2.01 ± 0.17 | 1.485 ± 0.014 | 8.2 ± 1.0 | 27.2 ± 1.2 | 1.45 ± 0.28 | $\rho = 2.87 \text{ g cm}^{-3}$, temp. 22°C $B_1^2 = 0.0048 \text{ cm}^{-2}$ $329 \leq \omega \leq 3140 \text{ rad sec}^{-1}$ |

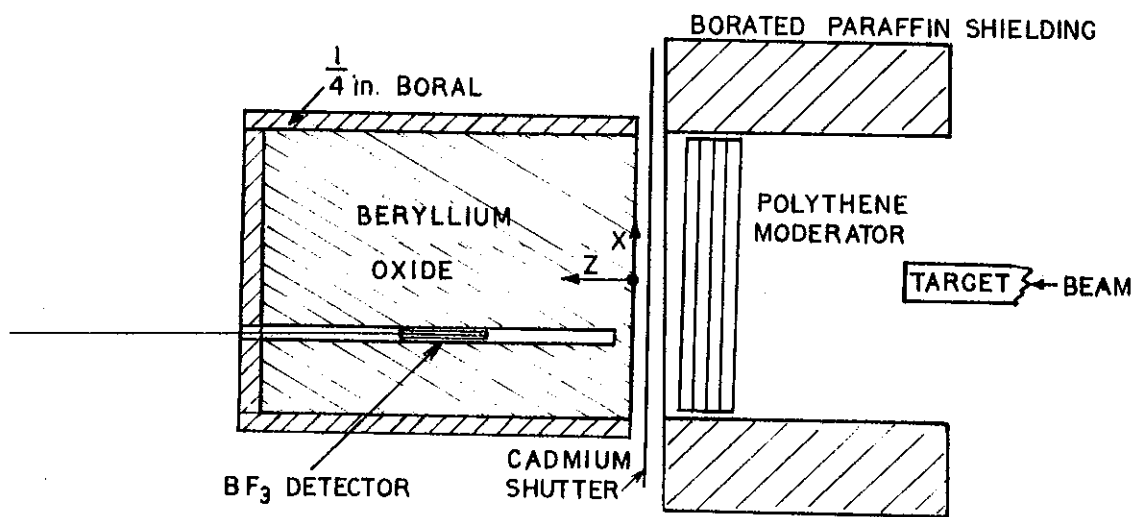


FIGURE 1. SCHEMATIC DIAGRAM OF NEUTRON SOURCE AND MODERATOR ASSEMBLY

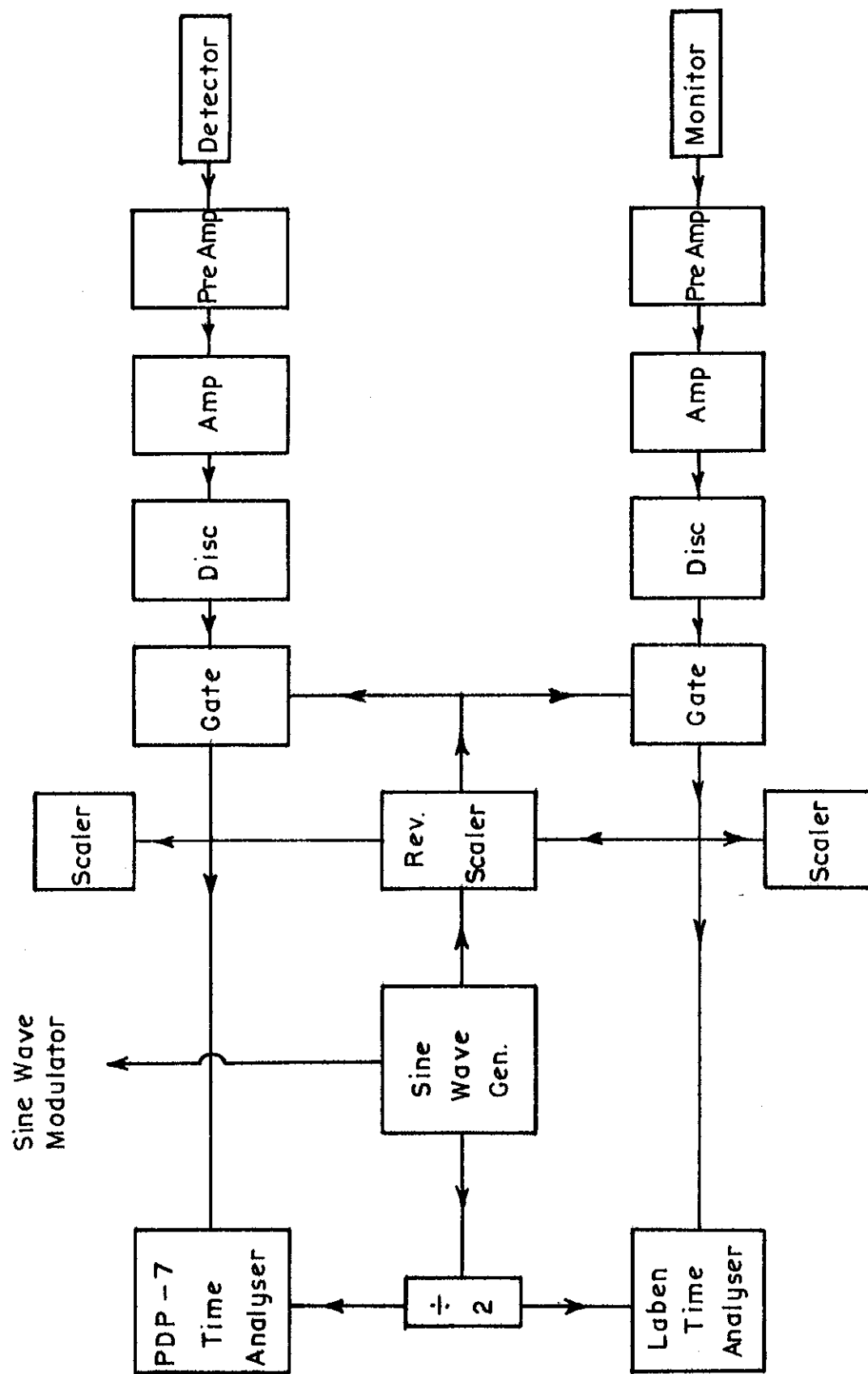


FIGURE 2. BLOCK DIAGRAM OF TIME ANALYSIS SYSTEM

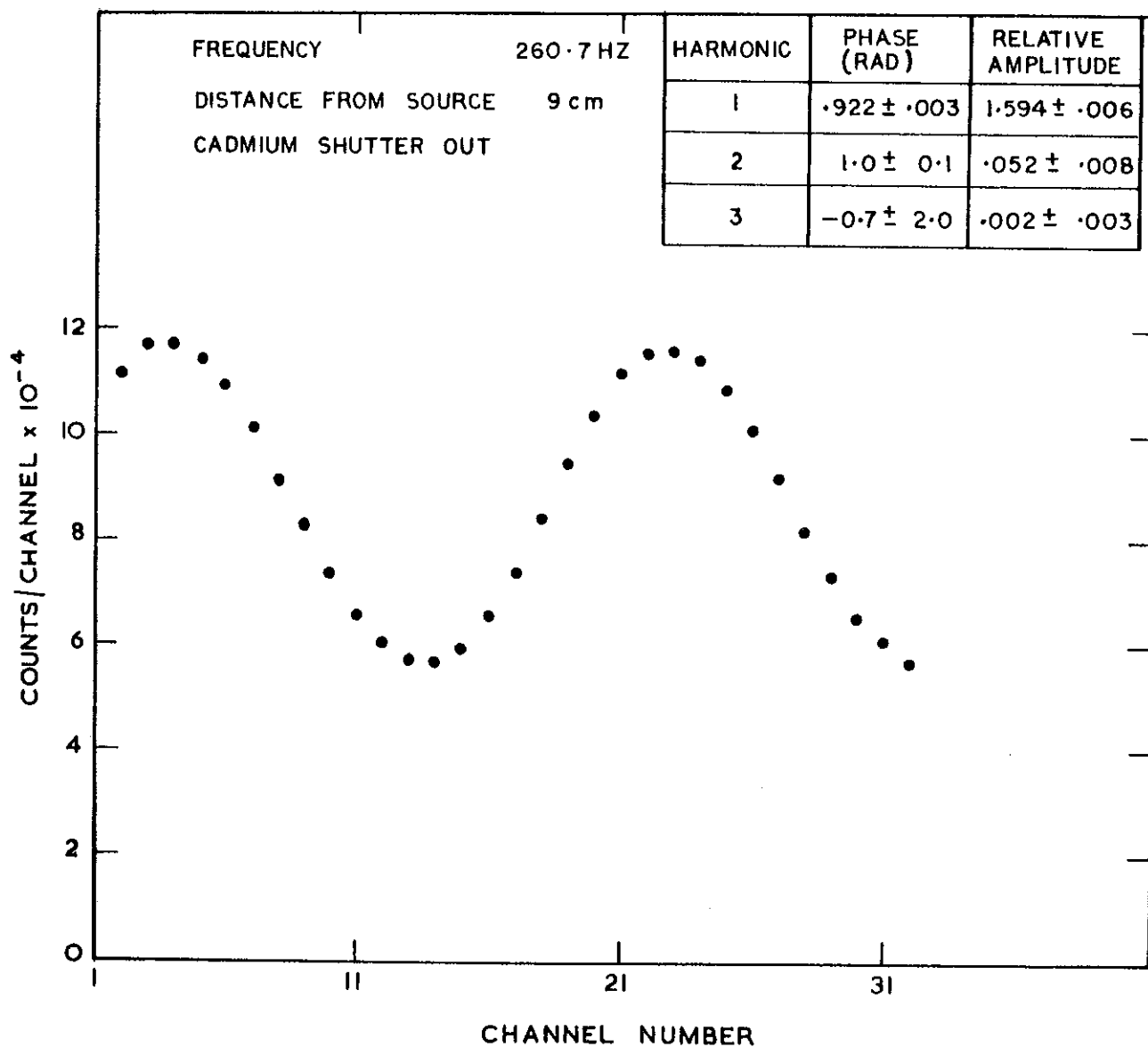


FIGURE 3. TYPICAL TIME DISTRIBUTION AND ITS HARMONIC ANALYSIS

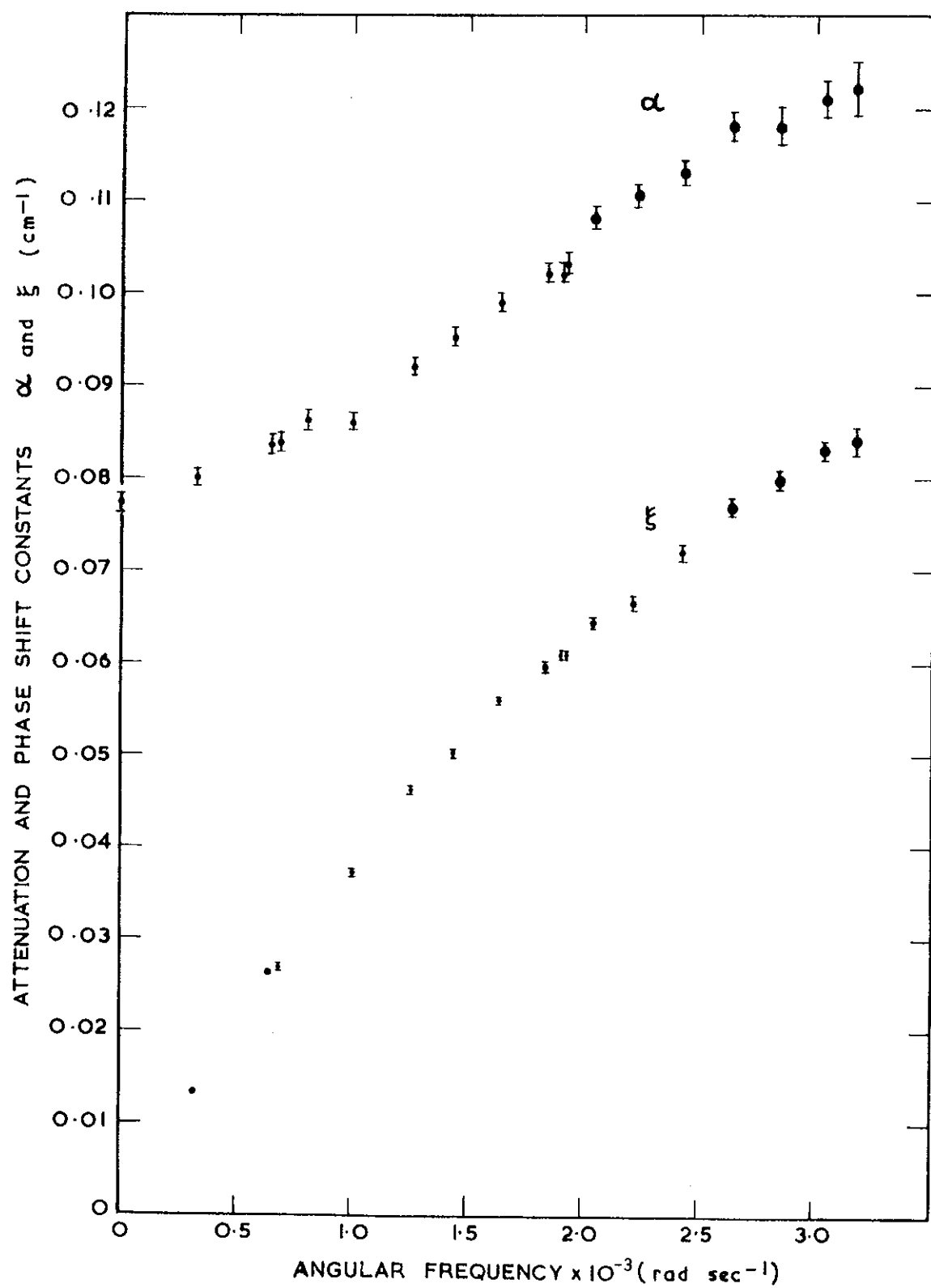


FIGURE 4. THE ATTENUATION CONSTANT α AND PHASE SHIFT CONSTANT ξ FOR BeO OF DENSITY 2.87 g cm^{-3} AS A FUNCTION OF THE ANGULAR FREQUENCY ω

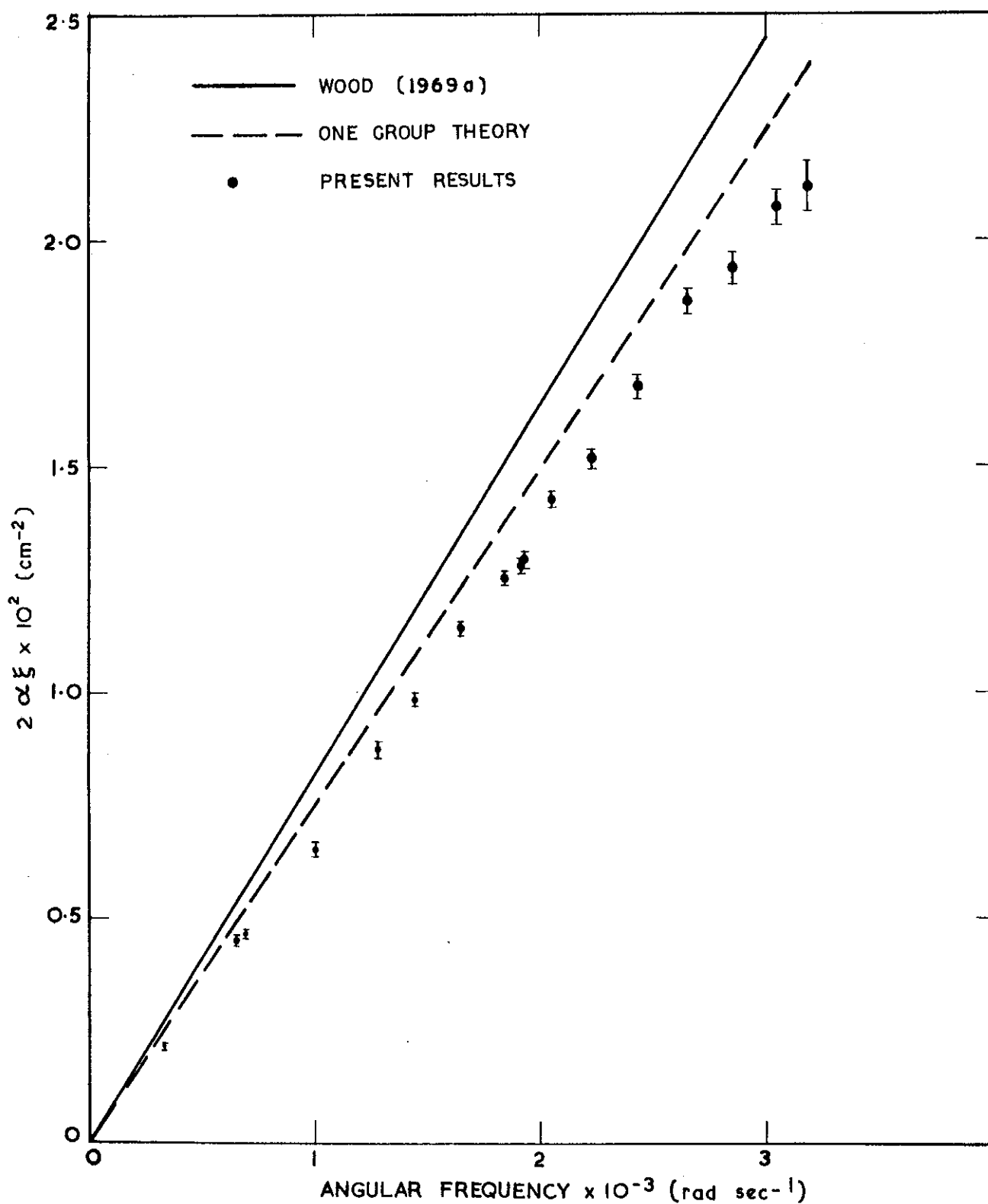


FIGURE 5. THE QUANTITY $2\alpha\xi$ FOR BeO, NORMALISED TO A DENSITY 2.96 g cm^{-3} , AS A FUNCTION OF THE ANGULAR FREQUENCY ω

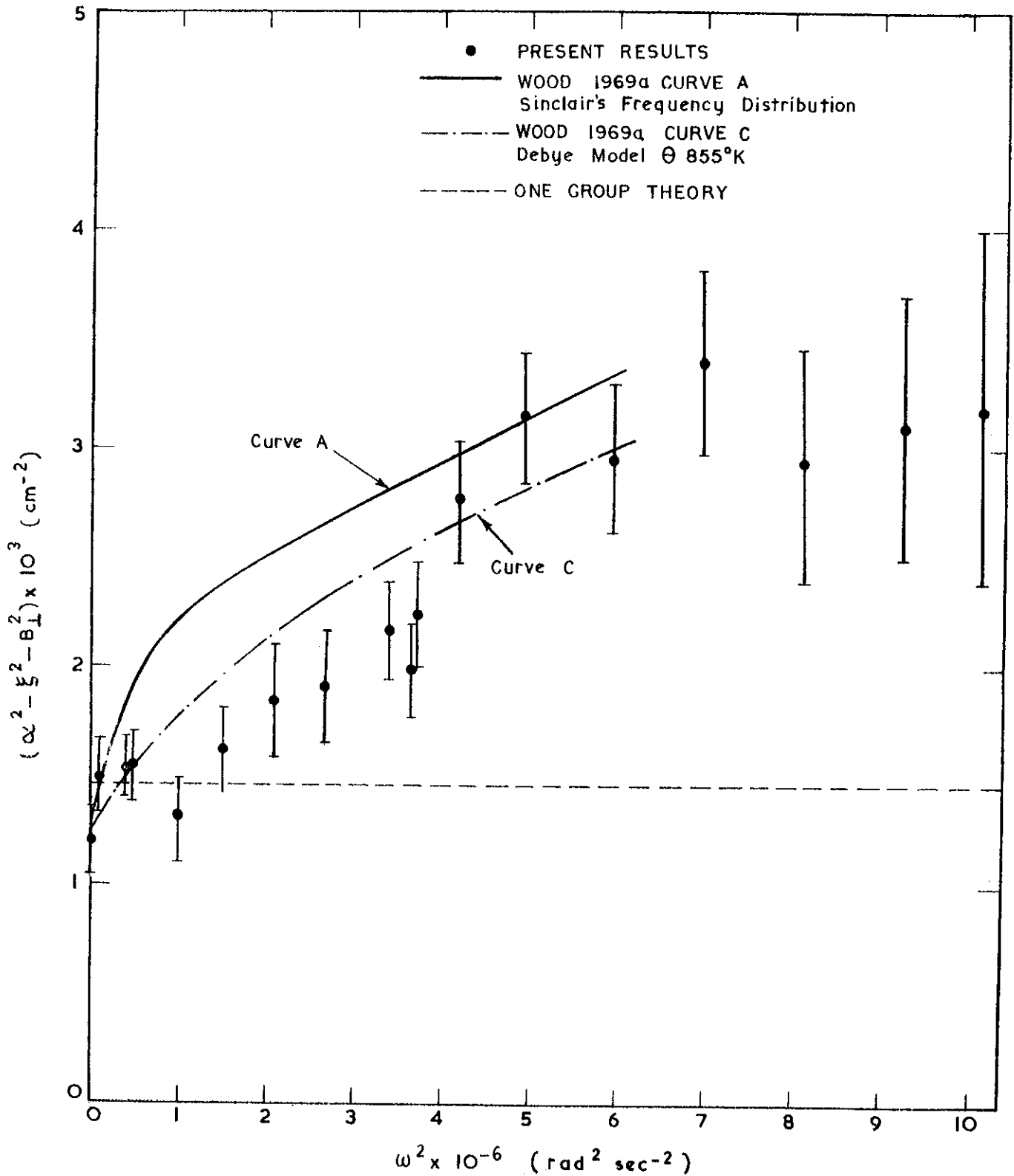


FIGURE 6. THE QUANTITY $\alpha^2 - \xi^2$ FOR BeO, NORMALISED TO A DENSITY 2.96 g cm^{-3} , AS A FUNCTION OF THE ANGULAR FREQUENCY ω .